Rev.Adv.Mater.Sci. 21(2009) 200-204

THE EFFECT OF HEAT TREATMENT TEMPERATURE ON CeO_2 AND Y_2O_3 DOPED CeO_2 ELECTROSPUN FIBERS

A.K. Alves[1,2], F. A. Berutti[1,2], F. Clemens[2], T. Graule[2] and C. P. Bergmann[1]

[1] Federal University of Rio Grande do Sul, Av. Osvaldo Aranha, 99 sala 705C. 90035-190 Porto Alegre – RS, Brazil

[2] Laboratory of High Performance Ceramics, EMPA, Ueberlandstrasse 129 CH-8600 Duebendorf, Switzerland

Received: June 06, 2008

Abstract. Electrospinning was employed to produce homogeneous inorganic–organic composite fibers from alcoholic solutions containing polyvinyl butyral (PVB) and precursor of yttrium and cerium ions. Upon heat treatment, ceria and yttria-doped ceria fibers were obtained. The fibers retained the original morphology observed in the as-spun composition. X-ray diffraction was used to identify the crystalline phases of the final products. Scanning electron microscopy (SEM), thermogravimetric analysis (TGA), differential thermal analysis (DTA), and BET analysis were employed to study the ceramic-phase formation and the morphological evolution of the fibers. Thus, several micrometers long, uniform ceria and yttria-doped ceria fibers of high-phase purity were produced. The CeO_2 and the CeO_2 with Y_2O_3 fibers presented average diameter that ranged from 19 to 25 μm, and the distribution of specific surface ranged from 33 to 43 m^2/g.

1. INTRODUCTION

Cerium oxide has been employed extensively in catalytic combustion as a catalyst or as a textural and structural promoter for supported metal or metal-oxide catalysts [1-2]. The main advantage of using catalysts in conventional flame combustion processes is that they simultaneously suppress NO_x emission and improve energy efficiency [3-6].

Generally, the structural promotion effect is attributed to the capability of the cerium to form crystalline oxides with lattice defects, which may act as catalytic active sites [7], whereas its textural promotion effect is given by the excellent thermal and mechanical resistance which CeO_2 confers to catalysts [7–11].

An interesting property of CeO_2 is its ability to release and absorb oxygen during alternating redox conditions, and hence to function as a oxygen buffer [12-13]. The addition of dopants can increase the concentration of oxygen vacancies and improve the thermal stability of the parent oxide [13]. Cerium and yttrium mixed-oxide formulations are used as a catalyst for reforming and for the partial oxidation of methane [14].

A method that can be used to produce nanomaterials is electrospinning. This technique uses external electrical forces to produce polymeric fibers of diameters in the range of 3 to 1000 nm, depending upon the strength of the applied voltage between a drop of the precursor solution (or melt) and the collecting surface. The possibility of extending this concept to ceramic systems has opened a new era in nanostructure research during the past couple of years [15-18].

In this study, CeO_2 and different amounts of Y_2O_3 added to CeO_2 fibers were prepared by electrospinning method. The compositions were first electrospun in the form of polymer-inorganic salt composite which were subsequently processed to yield the desired ceramic composition. The trans-

Corresponding author: A.K. Alves, e-mail: annelika@gmail.com

© 2009 Advanced Study Center Co. Ltd.

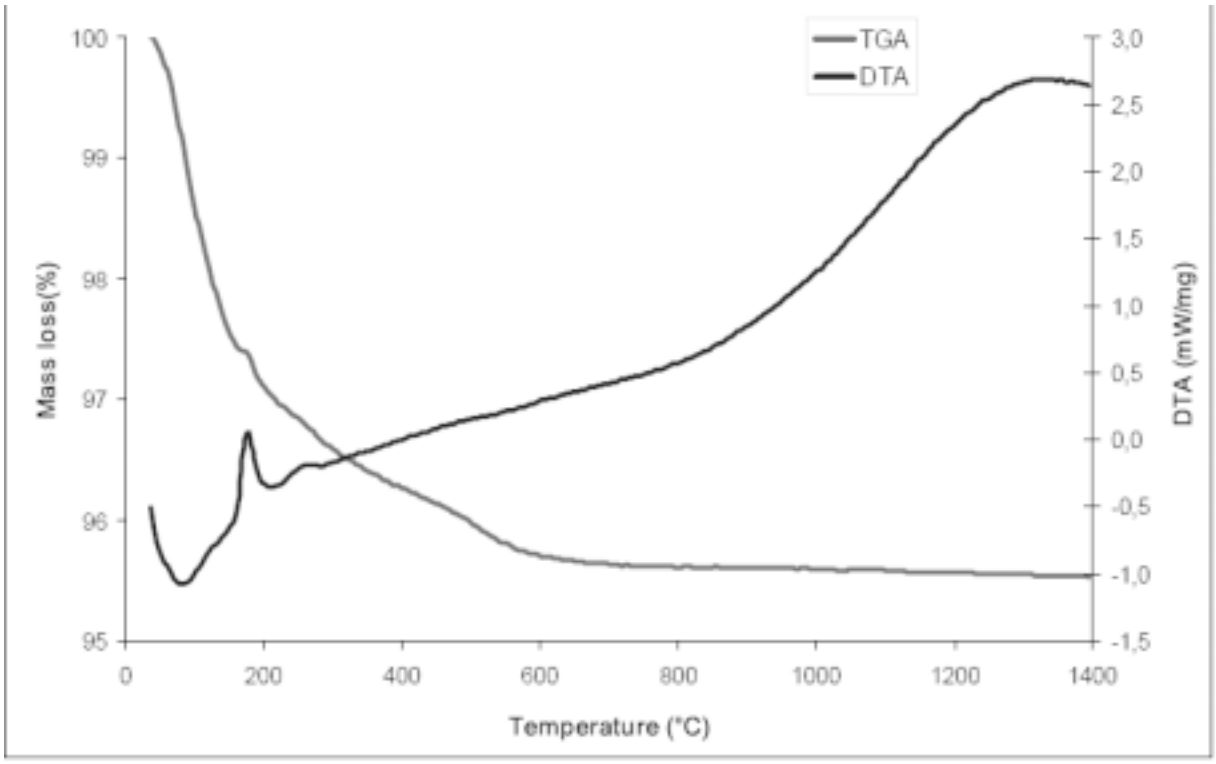

Fig. 1. TGA/DTA plot of PVB-cerium nitrate composite fibers in air at 10 °C/min.

formation of the composite to ceramic was verified by TGA/DTA, XRD, BET, and SEM techniques.

2. EXPERIMENTAL

Analytical-grade $Ce(NO_3)_3 \cdot 6H_2O$ (=99% Sigma-Aldrich), $Y(NO_3)_3 \cdot 6H_2O$ (=99.99% Sigma-Aldrich), anhydrous ethanol, and polyvinylbutyral (PVB-B20H, Clariant) were used as raw materials. A gel synthesis method was used to prepare the CeO_2 and the CeO_2-Y_2O_3. The precursors $Ce(NO_3)_3 \cdot 6H_2O$ and $Y(NO_3)_3 \cdot 6H_2O$ were weighed according to the molar ratio to achieve the following compositions: CeO_2, $Ce_{0.9}Y_{0.1}O_{1,95}$, $Ce_{0.7}Y_{0.3}O_{1,85}$, $Ce_{0.5}Y_{0.5}O_{1,75}$, $Ce_{0.3}Y_{0.7}O_{1,65}$, and $Ce_{0.1}Y_{0.9}O_{1,55}$.

The salts were first dissolved in ethanol and then mixed together with 20 g of a 20 wt.% PVB ethanol solution. The translucent solutions were evaporated at 60°C for 1 h under stirring to form a viscous gel. The system was homogenous during the preparation of the gels, and no precipitation was observed. These viscous gels were aged for 24 h at room temperature to achieve the correct viscosity for the electrospinning process, approximately 125 cP.

The electrospinning apparatus consisted of a syringe infusion pump (Model A-99, Razel Scientific Instruments), a high voltage power supply (EH-Series, Glassman High Voltage), and a cylindrical grounded counter electrode. The gel was loaded into a 5-mL syringe and an electrode is clipped onto a 16-Gauge (inner diameter 1.49 mm) stainless-steel needle. The flow rate of solution to the needle tip was maintained so that a pendant drop remains during electrospinning. All air bubbles were eliminated and the solution was electrospun between 5 and 17 kV horizontally onto the target. The grounded rotational cylindrical counter electrode, covered with an aluminum foil, was between 10 and 20 cm apart from the charged needle. The concentration, viscosity, conductivity of the solution as well as the applied voltage and the distance between the charged electrode and the grounded target were adjusted in order to obtain a stable jet.

The fibers thus formed on the aluminum foil were dried initially at 60 °C for 24 h. And then, the fibers were heat treated at 500 °C for 3 h, with a heating rate of 40°C/h. To achieve a higher crys-

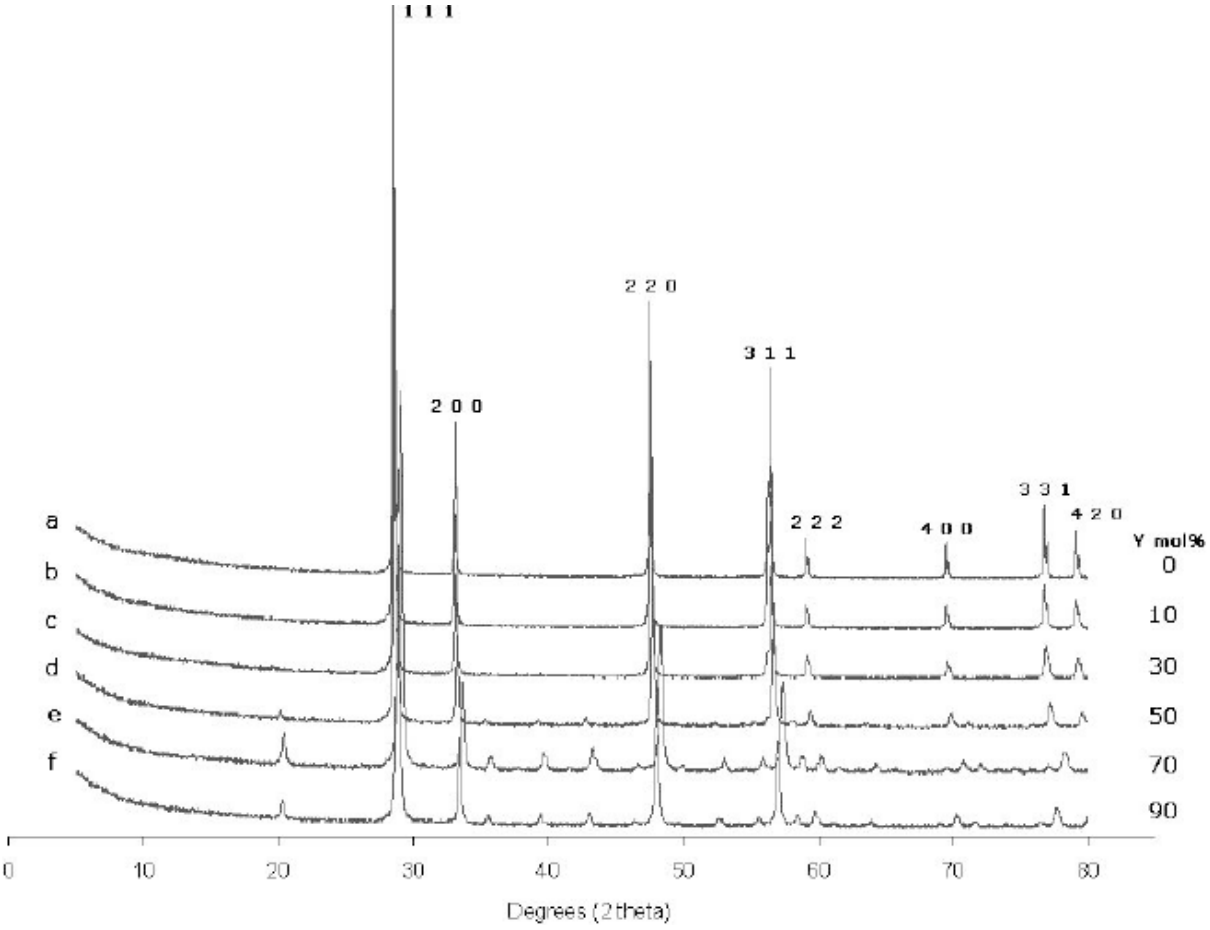

Fig. 2. X-ray diffraction profiles of heat-treated fibers (1000 °C): (a) CeO_2, (b) $Ce_{0.9}Y_{0.1}O_{1,95}$, (c) $Ce_{0.7}Y_{0.3}O_{1,85}$, (d) $Ce_{0.5}Y_{0.5}O_{1,75}$, (e) $Ce_{0.3}Y_{0.7}O_{1,65}$, and (f) $Ce_{0.1}Y_{0.9}O_{1,55}$.

tallinity, the fibers were further treated at a temperature range between 500 and 1000 °C for 3 h at the same heating rate.

Simultaneous TG/DTA (NETZSCH STA409C) experiments were performed on the as-obtained fibers in order to study the thermal behavior. The samples were heated up to 1100 °C at a heating rate of 10 °C/min in a flowing air atmosphere. Phase analysis of the heat-treated fibers was performed using the powder X-ray diffraction method (PANalytical B.V XRD; X'Pert Pro MPD). Measurements were conducted with Cu *K*a radiation (40 mA filament current, 40 kV accelerating voltage). Curve fitting and integration were carried out using Philips X'Pert high score plus. The specific surface area (S_{BET}, m^2g^{-1}) of the heat-treated fibers were measured using the standard Brunauer–Emmett–Teller (BET) technique with N_2 adsorption (Beckman Coulter SA3100). Before the measurement the samples were evacuated at 70 °C for 2 h. Microstructural analysis of the fibers were performed with a scanning electron microscope (SEM; Vega Plus TS 5136MM, TeScan,). Samples were mounted on aluminum sample holders with a carbon tape and sputtered with a gold–palladium alloy to prevent electrical charging during the SEM analysis.

3. RESULTS AND DISCUSSION

The typical TGA-DTA behavior of the as-spun composite fibers is shown in Fig. 1, here exemplified as the behavior of the composite PVB-$Ce(NO_3)_3$. Similar DTA/TG curves were also observed with different amounts of yttrium nitrate. From Fig. 1, it can be observed that most of the organic materials such as PVB, ethanol, nitrates, and the other volatiles were removed at temperatures below

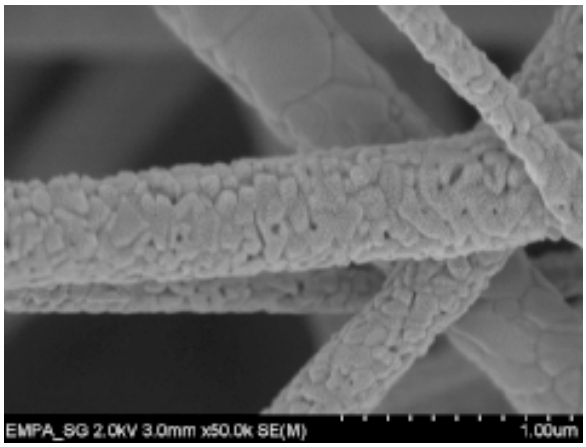

Fig. 3. High-resolution SEM image of CeO_2 fibers heat treated at 1000 °C.

700 °C. The peak at 100 °C of the DTA curve correspond to the loss of adsorbed moist and the peaks at around 190 and 265 °C correspond to the decomposition of nitrates and also to the degradation of PVB, which has two degradation mechanisms involving both intra- and intermolecular transfer reactions [19].

The XRD pattern of the composite fibers heat treated at 1000 °C is shown in Fig. 2. At this treatment temperature, all the samples show the crystal structure of CeO_2 or Y_2O_3 solid solution. A change in the composition results in a change in the crystal structure. For the compositions $Ce_{0.5}Y_{0.5}O_{1,75}$, $Ce_{0.3}Y_{0.7}O_{1,65}$, and $Ce_{0.1}Y_{0.9}O_{1,55}$ in Fig. 2, peaks at about 2θ = 20, 37, 40, and 43° show the lattice formation of Y_2O_3, as a main phase. With an yttrium oxide content of 30 mol.% and less, the peaks reveal a CeO_2 crystal structure.

The morphology of the nanofibers was examined by scanning electron microscopy (SEM). The average diameter of the fibers was analyzed from the SEM image using the software *UTHSCSA Image Tool*. At least 30 different fibers were measured for each condition. Fibers of CeO_2 obtained after the electrospinning process present an average diameter of 1.70 μm. After heat treatment at 1000 °C for 3 h the average diameter of the fibers is in the range of 0.80 μm. In general, metal oxide/polymer composite fibers were considerably shrunk by thermal treatment [20]. A shrinkage which causes a reduction in fiber diameter, observed between the spun fiber and the heat-treated fiber, is due to the mass loss of the organic components and to the beginning of the sintering process. Fig. 3 shows a high-resolution SEM image from the CeO_2 fiber mat heat treated at 1000 °C. It is noticed that the grains that build the fibers possess some porosity.

Table 1. Effect of the composition on the surface area and calculated amount of nitrates.

	S_{BET} (m^2/g)	Calculated NO_3 (g)
CeO_2	2.4	4,69697
$Ce_{0.9}Y_{0.1}O_{1.95}$	4.0	6,25027
$Ce_{0.7}Y_{0.3}O_{1.85}$	4.9	9,35705
$Ce_{0.5}Y_{0.5}O_{1.75}$	6.2	12,46362
$Ce_{0.3}Y_{0.7}O_{1.65}$	11.8	15,57019
$Ce_{0.1}Y_{0.9}O_{1.55}$	12.7	18,67697

Surface area of the electrospun fibers after heat treatment at 1000° C was determined using the BET method. Table 1 shows the BET results and the fiber diameter after heat treatment at 1000 °C.

In the heat-treatment process, the nitrates decompose via an exothermic reaction [21]. Due to the increasing amount of nitrates added, as shown in Table 1, it is expected that the gas formation will be greater, leading to higher surfaces areas in the compositions with higher amounts of nitrates. Heterogeneous catalysis reactions occur mainly on the surface of the catalyst. Thus, it is very important to have such material with the higher surface area as possible, since this area is associated with the presence of active sites, leading to increase in the rate of the reaction.

4. CONCLUSION

Fibers with diameters in the range of 0.2–0.5 μm have been successfully prepared by heat treating electrospun PVB-$Ce(NO_3)_3$ and PVB-$Ce(NO_3)_3$/$Y(NO_3)_3$ composite fibers. The fibers made of $Ce_{0.3}Y_{0.7}O_{1.65}$ and $Ce_{0.1}Y_{0.9}O_{1.55}$ show better resistance to heat treatment at 1000 °C, since they presented higher surface areas than the others. Fiber with a high yttrium content crystallize in Y_2O_3 crystal phase and have a specific surface area of around 12 m^2/g after being heat treated at 1000 °C for 3 h. So these fibers may have potential applications in catalyst combustion with high catalytic activity due to their high surface area and small pore size.

ACKNOWLEDGEMENT

The present work is supported financially by CNPq-Brazil (project no. 200506/2006-4) and EMPA-Switzerland.

REFERENCES

[1] A . Trovarelli, C. Leitenburg, M. Boaro and G. Dolcetti // *Catal. Today* **50** (1999) 353.
[2] J. Roggenbuck, H. Schäfer, T. Tsoncheva, C. Minchev, J. Hanss and M. Tiemann // *Microporous Mesoporous Mater*. **101** (2007) 335.
[3] L.F. Liotta, G. Di Carlo, G. Pantaleo and G. Deganello // *Catal Commun* **6** (2005); 329.
[4] D.L. Trimm // *Appl. Catal.* **7** (1983) 249.
[5] R. Prasad, L.A. Kennedy and E. Ruckenstein // *Catal Rev-Sci Eng* **26** (1984) 1.
[6] L.D. Pfefferle and W.C. Pfefferle // *Catal. Rev.-Sci. Eng* **29** (1987) 219.
[7] H. Xu, H. Yan and Z. Chen //. *J Power Sources* **163** (2006) 409.
[8] Y.F. Yu-Yao and J.T. Kummer // *J Catal* **106** (1987) 307.
[9] H.C. Yao and Y.F. Yu-Yao // *J Catal* **86** (1984) 254.
[10] T. Bunluesin, R.J. Gorte and G.W. Graham // *Appl Catal B* **14** (1997) 105.
[11] G.W. Graham, H.W. Jen and R.W. McCabe // *Catal Lett* **44** (1997) 185.
[12] E. Aneggi, M. Boaro, C. Leitenburg, G. Dolcetti and A. Trovarelli // *J Alloys Compd* **408** (2006) 1096.
[13] J. Papavasiliou, G. Avgouropoulos and T. Ionnides // *App Catal B Envir* **69** (2007) 226.
[14] S. Colussi, C. Leitenburg, G. Dolcetti and A. Trovarelli // *J Alloys Compd* **374** (2004) 387.
[15] A.M. Azad // *Materials Letters* **26** (2006) 67.
[16] D. Li and Y. Xia // *Adv Mater* **26** (2004) 1151.
[17] S. Choi, B. Chu, S.G. Lee, S.W. Lee, S.S. Im, S.H. Kim and J.K. Park // *J Sol-Gel Sci Technol* **30** (2004) 215.
[18] H. Guan, C. Shao, Y. Liu, N. Yu and X. Yang // *Solid State Commun.* **131** (2004) 107.
[19] J.J. Seo, S.T. Kuk and K. Kim // *J Power Sources* **69** (1997) 61.
[20] W.K. Son, D. Cho and W.H. Park // *Nanotechnology* **17** (2006) 439.
[21] R.D. Purohit, S. Saha and A.K. Tyagi // *J Nuc Mater* **288** (2001) 7.